Proc. Natl. Acad. Sci. USA
Vol. 95, pp. 3269–3274, March 1998
Neurobiology

Multiple neurological abnormalities in mice deficient in the G protein G_o

MEISHENG JIANG*, MICHAEL S. GOLD*†, GUYLAIN BOULAY*, KARSTEN SPICHER*, MICHAEL PEYTON*‡, PHILIPPE BRABET§¶, YOGAMBUL SRINIVASAN§‖, UWE RUDOLPH§**, GAYLORD ELLISON††, AND LUTZ BIRNBAUMER*§,‡‡,§§,¶¶,‖‖

Departments of *Anesthesiology, ‡‡Biological Chemistry, §§Molecular, Cell and Developmental Biology, and ††Psychology, and ¶¶the Brain Research and Molecular Biology Institutes, University of California, Los Angeles, CA 90095; and §Department of Cell Biology, Baylor College of Medicine, Houston, TX 77030

Contributed by Lutz Birnbaumer, December 31, 1997

ABSTRACT **The G protein G_o is highly expressed in neurons and mediates effects of a group of rhodopsin-like receptors that includes the opioid, α_2-adrenergic, M2 muscarinic, and somatostatin receptors. *In vitro*, G_o is also activated by growth cone-associated protein of M_r 43,000 (GAP43) and the Alzheimer amyloid precursor protein, but it is not known whether this occurs in intact cells. To learn about the roles that G_o may play in intact cells and whole body homeostasis, we disrupted the gene encoding the α subunits of G_o in embryonic stem cells and derived G_o-deficient mice. Mice with a disrupted α_o gene ($\alpha_o-/-$ mice) lived but had an average half-life of only about 7 weeks. No $G_o\alpha$ was detectable in homogenates of $\alpha_o-/-$ mice by ADP-ribosylation with pertussis toxin. At the cellular level, inhibition of cardiac adenylyl cyclase by carbachol (50–55% at saturation) was unaffected, but inhibition of Ca^{2+} channel currents by opioid receptor agonist in dorsal root ganglion cells was decreased by 30%, and in 25% of the $\alpha_o-/-$ cells examined, the Ca^{2+} channel was activated at voltages that were 13.3 ± 1.7 mV lower than in their counterparts. Loss of α_o was not accompanied by appearance of significant amounts of active free $\beta\gamma$ dimers (prepulse test). At the level of the living animal, G_o-deficient mice are hyperalgesic (hot-plate test) and display a severe motor control impairment (falling from rotarods and 1-inch wide beams). In spite of this deficiency, $\alpha_o-/-$ mice are hyperactive and exhibit a turning behavior that has them running in circles for hours on end, both in cages and in open-field tests. Except for one, all $\alpha_o-/-$ mice turned only counterclockwise. These findings indicate that G_o plays a major role in motor control, in motor behavior, and in pain perception and also predict involvement of G_o in Ca^{2+} channel regulation by an unknown mechanism.**

G_o is an $\alpha\beta\gamma$ heterotrimeric G protein discovered in 1984 in brain by Neer and collaborators (1, 2) and by Sternweis and Robishaw (3), who all characterized it as a substrate for the ADP-ribosyltransferase activity of pertussis toxin. G_o has received special attention for the following reasons: (*i*) It is the most abundant G protein in neurons, where it can constitute up to 2% of membrane protein (3). (*ii*) In addition to neurons, it appears to be expressed only on endocrine cells and heart, albeit at much lower levels comparable to those of the other heterotrimeric G proteins. (*iii*) G_o is activated not only by the same class of seven-transmembrane receptors that activate the inhibitory G proteins G_{i1}–G_{i3} (4–9) but also by at least two proteins that do not belong to the rhodopsin-like family of G protein-coupled receptors, GAP43, an intracellular growth cone-associated protein active in neurite outgrowth (10), and the Alzheimer amyloid protein precursor protein responsible for familial forms of this disease (11). (*iv*) Except for inhibition of neuronal Ca^{2+} channels, for which the mechanism of action of G_o has been elucidated at the molecular level and shown to be due to the interaction of its $\beta\gamma$ moiety with the α_1 subunit of the channel (6, 12–16), the mode of action of G_o is essentially unknown. Tests for an α_i-like function for α_o have failed (17, 18). Activated α_o has transformed NIH-3T3 cells (19) and activated mitogen-activated protein kinase activity in Chinese hamster ovary cells (20), phospholipase C in *Xenopus* oocytes, and K^+ channels in neurons (21, 22), but how these effects come about has not been established. In fact, there is scant knowledge of the gamut of effector systems that may be the target(s) of activated G_o.

Gene ablation in mice is a powerful yet technically complex approach to identify as yet unknown functions of proteins that become manifest in mutated animals and/or in cell lines derived from them. It has been applied to several G proteins with the following interesting results. G_{i2}-deficient mice were found to develop ulcerative colitis and adenocarcinomas, revealing an unexpected and as yet unexplained role of G_{i2} in the development of a chronic inflammatory response and very likely in lymphocyte homing to enteric epithelia (23, 24). Ablation of G_q revealed an essential role for this G protein in platelet activation, because G_q-deficient mice bleed and their platelets fail to be activated by physiologic activators such as collagen, thrombin, thromboxane, and ADP (25). Also the ablation of G_o has been reported (26). Live mice, homozygous for loss of α_o, were obtained showing that α_o is not essential for life in spite of the features that set it apart from other G proteins. Mice lacking G_o were not like wild-type mice, however. They had a generalized tremor of unknown etiology and died at a very early postnatal ages. At the cellular level, G_o-deficient mice displayed a loss of muscarinic inhibition of isoproterenol-stimulated cardiac L type Ca^{2+} currents. The latter finding was unexpected, given that the present view is

The publication costs of this article were defrayed in part by page charge payment. This article must therefore be hereby marked "*advertisement*" in accordance with 18 U.S.C. §1734 solely to indicate this fact.

Abbreviations: DRG, dorsal root ganglion; DAMGO, [D-Ala,*N*-MePhe^4,Gly-ol]enkephalin.

†Present address: Department of Oral–Cranial–Biological Sciences, Dental School, University of Maryland, 666 West Baltimore Street, Baltimore, MD 21201.
‡Present address: Department of Molecular Biology and Oncology, University of Texas Southwestern Medical Center, NA7.132, 6000 Harry Hines Boulevard, Dallas, TX 75235.
¶Present address: Centre National de la Recherche Scientifique–Institut National de la Santé et de la Recherche Médicale de Pharmacologie-Endocrinologie, Rue de la Cardonille, 34094 Montpellier Cedex 2, France.
‖Present address: Cardiovascular Research Institute, Box 0130, University of California, San Francisco, CA 94143.
**Present address: Institute of Pharmacology, University of Zurich, Winterthurstrasse 190, CH-8057 Zurich, Switzerland.
‖‖To whom reprint requests should be addressed at: Department of Anesthesiology, BH-612 CHS (MC 177820), University of California Los Angeles School of Medicine, 10833 Le Conte Avenue, Los Angeles, CA 90095-1778. e-mail:lutzb@ucla.edu.

that this channel in particular is insensitive to inhibition by a G protein-coupled pathway; specifically, it does not interact with G protein $\beta\gamma$ dimers that inhibit the neuronal non-L type Ca^{2+} channels (16, 27, 28).

We have also used homologous recombination in embryonic stem cells to abolish its expression. The most prominent but not necessarily the most important of our findings is that G_o-deficient mice develop a turning behavior as if afflicted by unilateral lesions of the central nervous system.

MATERIALS AND METHODS

Vector and Cell Development. The intron exon structure of the gene encoding α_o has been elucidated (refs. 29 and 30 and Fig. 1). The α_o gene was disrupted in embryonic stem cells with previously described procedures and selection markers [Rudolph *et al.* (23, 33)]. 129Sv genomic DNA was obtained from a P1 cosmid selected from a commercial library (Genome Systems, St. Louis) by PCR screening with oligonucleotides A and B (where A is 5′-GGACAGCCTGGATCGGATTGG, a fragment of the sense strand of α_o exon 5, and B is 5′-ACCTGGTCATAGCCGCTGAGT, a fragment of the antisense strand of α_o exon 6) as primers (amplified fragment, 940 bp). A 10.8-kb *Hin*dIII–*Sal*I fragment containing exons 5, 6, 7.2, and part of 8.2 was used to construct a targeting vector. The final vector had a pBSII backbone (Stratagene) and contained a 4.2-kb *Hin*dIII–*Bam*HI fragment separated from 2.1-kb *Bam*HI fragment of the α_o gene by a Pol I-neomycin selection cassette (ref. 34 and Fig. 1). The MC1-tk counter-selection marker was placed at the 5′ end (35). This vector was transfected by electroporation into AB2.2 embryonic stem cells (from Allan Bradley, Baylor College of Medicine), and candidate recombinant clones were selected by growth on leukemia inhibitory factor-producing SNL feeder layers (also from Allan Bradley) in the presence of G418 (active ingredient; GIBCO/BRL; 180 μg/ml) and 0.2 μM 1-(2-deoxy-2-fluoro-β-D-arabinofuranosyl)-5-iodouracil (Moravek Biochemicals, Brea, CA). All cells were grown in DMEM containing glucose (4.5 g/liter), 2 mM glutamine, 15% heat-inactivated fetal bovine serum (GIBCO/BRL), 1% 2-mercaptoethanol, penicillin (100 units/ml), and streptomycin (100 μg/ml) (GIBCO/BRL). Recombinant clones were identified by Southern blot analysis using a 1.2-kb *Bam*HI–*Xho*I 3′ external probe. After confirming the insertion of the Pol II-neomycin cassette into the *Bam*HI site of the α_o gene and absence of secondary insertions, the targeted 129Sv embryonic stem cells were injected into C57BL/6J blastocysts from which chimeric mice were derived. Two (129Sv × C57BL/6J) F_1 cross-bred mouse strains heterozygous for loss of $G_o\alpha$ were obtained from two chimeric (F_0) mice and these

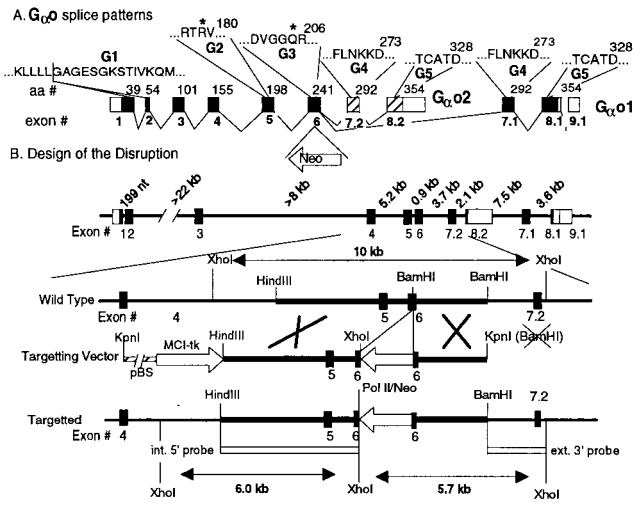

FIG. 1. Genomic organization of the gene encoding G_o α subunits and design of the disruption. (*A*) Intron–exon boundaries of the cDNA coding for $G_o\alpha$ and location of key amino acid sequences. Boxes, exons; open boxes, untranslated sequences; solid or hatched boxes, translated sequences. Exon numbering is shown below and the number of the last amino acid of each exon is shown above the cDNA. Amino acids in G1 through G5 regions are responsible for binding and hydrolysis of GTP (31). Mutations in R* and Q* of G2 and G3 reduce GTPase activity (32). Pertussis toxin (PTX) ADP ribosylates a Cys at position −4 from C terminus. (*B*) Genomic structure of the $G_o\alpha$ gene (29, 30), structure of the targeting vector, 3′ and 5′ probes for Southern blot analysis, and expected restriction fragment sizes of the wild-type and the mutated alleles.

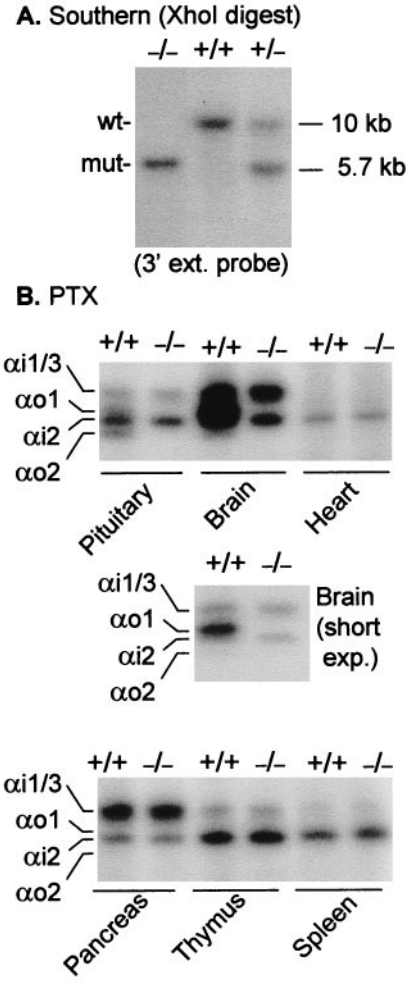

FIG. 2. Genotype and ADP-ribosylation patterns of wild-type and α_o−/− mice. (*A*) Southern blot analysis of *Xho*I-digested DNA from tail biopsies of −/− mice and +/− and +/+ littermates; the probe was the 3′ external probe shown in Fig. 1. (*B*) Selected tissues from wild-type mice and mice predicted by Southern blot analysis to be G_o-deficient. Homogenizations were all in 27% sucrose/1 mM EDTA/10 mM Tris·HCl, pH 7.5. Homogenates were ADP-ribosylated without further processing in the presence of guanosine 5′-[β-thio]diphosphate, adenosine 5′-[β,γ-imido]triphosphate, 0.1% SDS, and 2 mM DTT for 30 min at 32°C in a final volume of 15 μl as described (36). NAD was then added to give 4 mM, mixed with 30 μl of 2× Laemmli's sample buffer, and separated by urea-gradient SDS/PAGE in 9% gels (36). The gels were stained and destained over night and autoradiographed. Except for brain, the predominant bands are α_{i2}. Note that in the pituitary the intensities of α_{o1} and α_{o2} (above and below α_{i2}) are about equivalent; in brain, α_{o1} is the predominant band with $\alpha_{i1/3}$ and α_{i2} being similar in intensity. In heart ventricle homogenates, only the α_{i2} band is evident [absent in α_{i2}-deficient hearts (37)].

were bred to homozygosity (F_2 mice) for loss of $G_o\alpha$ ($\alpha_o-/-$ mice, Fig. 2*A*).

Genotyping. Southern blot analysis was performed according to Sambrook *et al.* (38) with DNA isolated from tail biopsies. The 3′ external probe was a 1.8-kb *Bam*HI–*Xho*I fragment, and the 5′ probe was the 4.2-kb *Hin*dIII–*Bam*HI fragment used to construct the vector. The plasmid pBluescript KSII, the PolII-Neo cassette and the MC1-tk cassette were used to probe for absence of these sequences in the targeted embryonic stem cell. Probes were labeled with [^{32}P]dCTP by using the random priming method (39). For hybridization, DNA digests were depurinated and transferred onto GeneScreen*Plus* membranes (NEN/Dupont). The filters were baked at 80°C under vacuum, washed for 1 h at 65°C with 2× SSC (1× SSC = 150 mM NaCl/15 mM sodium citrate, pH 7.0), and prehybridized in 0.5 M sodium phosphate/7% SDS/1% BSA/0.5 mM EDTA, pH 7.2, for 4–6 h at 65°C. Hybridization was at the same temperature in the same solution containing the heat-denatured probes at 2–10 × 10^6 cpm/ml. After 15 h, the filters were washed for four 5-min periods with 0.5× SSC/0.1% SDS at room temperature and for two 15-min periods at 65°C. The membranes were autoradiographed by using Kodak BioMax MR films. The PCR was also used to genotype DNA samples. Amplification conditions were 1 min at 94°C, 2 min at 64°C, and 3 min at 72°C for 35 cycles with oligonucleotides A and B for wild-type DNA (940 bp) and C and B for mutant DNA (where C is 5′-CAATGGCCGATCCCATATTGGCTGC, an antisense fragment located in the coding region of the neomycin gene; 700 bp) as primers.

Isolation of Dorsal Root Ganglion (DRG) Cells and Recording of Voltage-Gated Ca^{2+} Channel Currents. Sensory neurons were obtained from the lumbar and thoracic dorsal root ganglia of adult mice. Ganglia were enzymatically treated and mechanically dispersed as described (40), except that the ganglia were not desheathed and that collagenase treatment was 90 min. DRG neurons were plated onto laminin/ornithine-coated glass coverslips and incubated overnight in MEM containing 10% fetal bovine serum and mouse nerve growth factor (2.5 S; 10–20 ng/ml) at 37°C, 90% humidity, and 3% CO_2 before recording.

Voltage-clamp recordings were performed within 30 h of plating by using an Axopatch 200A amplifier (Axon Instruments, Foster City, CA) in the whole-cell patch configuration as described (39). Data were filtered with a 4-pole Bessel filter and digitized. Series resistance, 0.3–5 MΩ, was estimated from the settling rate of the voltage clamp and the membrane capacitance and was compensated (>80%) by using amplifier circuitry. Only data obtained from neurons in which uncompensated series resistance resulted in voltage-clamp errors of less than 5 mV were used. A P/4 protocol was used for leak subtraction. To ensure the linearity of leakage currents around the holding potential for the P/4 protocol, the resting conductance for each cell was determined at potentials between −100 and −60 mV. Data were fit with a nonlinear least-square method.

Ba^{2+} was used as the charge carrier. The bath solution contained 130 mM choline chloride, 2.5 mM $BaCl_2$, 0.6 mM $MgCl_2$, 10 mM Hepes, and 10 mM glucose (pH was adjusted to 7.4 with Tris base and osmolarity was adjusted with sucrose to 325 milliosmolar). The electrode solution contained 140 mM CsCl, 0.1 mM $CaCl_2$, 2 mM $MgCl_2$, 11 mM EGTA, 10 mM Hepes, 2 mM Mg-ATP, and 1 mM Li-GTP (pH was adjusted to 7.2 with Tris base and osmolarity was adjusted with sucrose to 310 milliosmolar). Patch pipettes filled with electrode solution had resistances of 2–6 MΩ.

Whole-cell impedance and capacitance of each cell were estimated by stepping the membrane potential to −90 mV for four 10-ms periods and measuring the area under the transient associated with the voltage step. Ba^{2+} currents were evoked from a holding potential of −70 mV by 40-ms steps to 0 mV every 10 s. Currents were sampled at 50 kHz and filtered at 5 kHz. [D-Ala,*N*-MePhe^4,Gly-ol]Enkephalin (DAMGO at 1 μM, dissolved in bath solution; from Research Biochemicals) was applied for 1–2 min, and its effect was determined as a percent change in peak evoked current (39) or, with a prepulse potentiation protocol, as an increase in peak current after a depolarizing step to +80 mV for 100 ms (prepulse) preceding a 30-ms test depolarization to −5 mV initiated 10 ms after the end of the prepulse. Conductance–voltage curves were constructed for each neuron from instantaneous tail currents evoked at −70 mV after 40-ms voltage steps between −80 and +50 mV taken at every 5 mV. Current density was estimated by dividing the peak current evoked at the start of the experiment by the cell capacitance and did not differ in neurons from $\alpha_o+/+$ and $\alpha_o-/-$ mice (data not shown).

ADP Ribosylation of Membrane Particles from Murine Tissues. Except for heart, all other homogenates were made in Dounce homogenizers and 27% (wt/wt) sucrose/1 mM EDTA/10 mM Tris·HCl, pH 7.5. Homogenates were centrifuged in glass tubes for 5 min at 1,000 × *g*, the loose pellets were discarded, and membranes to be ADP-ribosylated were collected by centrifugation at 12,000 × *g* for 20 min. Cardiac tissue was homogenized in the same medium but with a Polytron at a setting of 8 for 60 s. A pellet, obtained by centrifuging at 10,000 × *g* for 20 min, was discarded, and membranes to be ADP-ribosylated were collected by centrifugation at 100,000 × *g* for 30 min in a Beckman SW 50.1 rotor. Other procedures used to ADP-ribosylate and separate the ADP-ribosylated proteins by urea and polyacrylamide gradient gel electrophoresis (urea-gradient SDS/PAGE) were as described (40).

Adenylyl cyclase activity was assayed in murine ventricular heart muscle homogenates as described (41).

RESULTS AND DISCUSSION

Disruption of the Gene Encoding α_o Variants. Two G_o α subunit cDNAs, derived from alternatively spliced mRNAs, have been identified by molecular cloning: α_{o1}, encoded in exons 1 through 6 plus 7.1, 8.1, and 9 (42–44); and α_{o2}, encoded in exons 1 through 6 plus 7.2 and 8.2 (45, 46). α_{o1} and α_{o2} differ in 26 amino acids dispersed along their last 111 amino acids (total length, 354 amino acids; Fig. 1*A*). In urea-gradient SDS/PAGE gels, ADP-ribosylated α_{o1} migrates very close but slightly behind ADP-ribosylated α_{i2}, which it often occludes, and ADP-ribosylated α_{o2} migrates slightly ahead of ADP-ribosylated α_{i2} (47). A posttranslational modification of unknown nature generates a third α_o (α_{oC}) that comigrates in SDS/PAGE gels with α_{o2} (47, 48). Fig. 1 shows the intron–exon organization of the $G_o\alpha$ gene (29, 30) and the structural features of the insertion vector constructed to disrupt this gene. The neomycin selection cassette was inserted into exon 6, which is common to both splice variants, and thus prevents synthesis of all forms of G_o.

Intercrosses of +/− mice yielded G_o-deficient mice ($\alpha_o-/-$ mice). $\alpha_o-/-$ mice had DNA with the expected restriction endonuclease pattern (e.g., Fig. 2*A*) and, by ADP ribosylation of brain, pituitary, pancreatic islet, and cardiac membranes, showed the expected loss of G_o proteins (Fig. 2*B*). No difference in ADP-ribosylation pattern was seen in tissues not expressing $G_o\alpha$ (e.g., thymus, spleen, liver, lung, and exocrine pancreas). A comparison of the pituitary and brain ADP-ribosylation patterns clearly shows that, relative to α_{o1}, α_{o2} is more abundant in the pituitary.

$\alpha_o-/-$ Mice: Inheritance of the Disruption and Poor Survival. Thirty-eight embryos resulting from four +/− × +/− crosses were genotyped at embryonic days 18–20. We found 8 −/−, 14 +/−, and 15 +/+ mice (22, 38, and 40%, respectively), indicating an under-representation of embryos with one or two disrupted alleles (χ^2 test, $P > 0.05$). Loss of

−/− mice became very noticeable after birth. Thus, at weaning we had 348 live mice from 46 litters: 21 −/−, 177 +/−, and 105 +/+ mice, for a distribution of 7, 58, and 35%, respectively. This distribution indicates early death of −/− mice. Also, 3-week-old −/− animals are small, with a mean body weight that is only 45% the weight of their littermates. Weaned −/− animals are unable to feed well by themselves in standard cages either because of the small size or because of general weakness. However, they eat food supplied as a paste on a dish and, those that survive, grow well so that by 8 weeks they have a body weight that does not differ from that of their littermates (Fig. 3*A*). Weight and growth characteristics of α_o+/− mice are indistinguishable from those of wild-type littermates. Fig. 3*B* shows the survival curve of 31 α_o−/− mice starting after the first postnatal week; by 7 weeks 50% had died of unknown reasons. Two survived for more than 50 weeks. When subjected to hot-plate tests, α_o−/− animals were found to be hyperalgesic (Fig. 3*C*). This suggests a role for a G_o-coupled pathway in normal pain perception.

Ca^{2+} Current in Sensory DRG Cells of α_o−/− Mice: Inhibition by Opioid Receptor and Activation by Voltage. G_o has been implicated as a mediator of negative feedback regulation of presynaptic Ca^{2+} channels (13), and the spinal analgesic effect of opioids has been proposed to be due, at least in part, to inhibition of presynaptic Ca^{2+} channels in the afferent pathway. This was based on the ability of opioids to inhibit the evoked release of neurotransmitter (49) and their ability to inhibit neuronal Ca^{2+} channels thought to be located at presynaptic terminals (27). We thus tested whether opioid-receptor-mediated inhibition of Ca^{2+} currents in sensory DRGs would be affected by loss of G_o. As shown in Fig. 4, lack of G_o resulted in a partial (30%, $P < 0.05$) loss of the inhibitory effect of the μ-selective opioid receptor agonist DAMGO. This indicates that inhibition of these type of currents is not solely mediated by G_o (Fig. 4). We noted further that in 7 of 31 α_o−/− cells examined, the position of the conductance–voltage relationship was shifted by −13.3 ± 1.7 mV. Whether the combination of the reduced response to G_i/G_o-coupled receptors and the shift in activation voltage are related to and/or responsible for the hyperalgesia seen in hot-plate tests or whether the hyperalgesia is rooted in some other change(s) in neuronal sensitivity remains to be determined.

The opioid receptor-induced inhibition of neuronal non-L type Ca^{2+} currents is thought to be the direct consequence of the $\beta\gamma$ dimer of G_o interacting with the α_1 Ca^{2+} channel subunit (for review, see ref. 50; see also ref. 16). The "prepulse facilitation" protocol was applied to test whether the inhibition seen in the absence of G_o was still mediated by $\beta\gamma$ dimers. This test is based on the observation that inhibition of Ca^{2+} current by the δ-opioid receptor in NG108–15 cells is very pronounced at low test potentials, −20 to 0 mV, but wanes at higher test potentials (12). This phenomenon is common for the effects of G_i/G_o-coupled receptors including the type B γ-aminobutryic acid receptor in chicken DRG cells (51) and the α_2-adrenergic

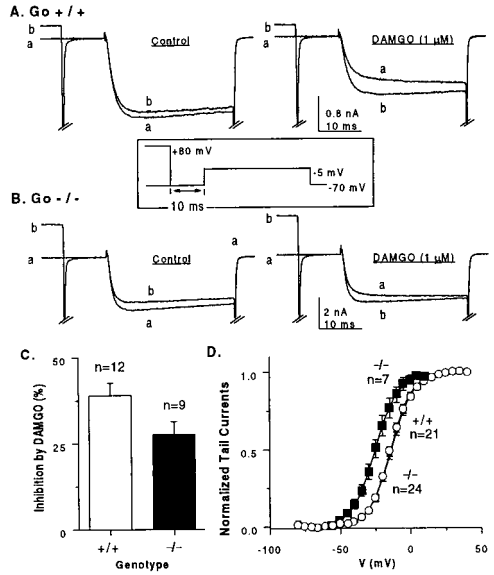

FIG. 4. Ca^{2+} current regulation in DRG cells from α_o−/− mice and α_o+/+ littermates. (*A*) α_o+/+ cells. (*Left*) Lack of a depolarizing prepulse to potentiate Ca^{2+} channel current elicited by a test pulse to −5 mV. (*Right*) Reversal by prepulse of opioid receptor-mediated inhibition of Ca^{2+} channel current. (*B*) α_o−/− cells. (*Left* and *Right*) As in *A*. (*Inset*) Voltage protocol used in *A* and *B*. (*C*) Means of opioid inhibition of Ca^{2+} channel current in α_o−/− and α_o+/+ cells. Inhibition by DAMGO was 39 ± 3.6% for +/+ and 27.6 ± 3.8 for −/− cells. The difference, 11.4 ± 5.2%, is significant at the $P < 0.05$ level. (*D*) Current–voltage relationship of Ca^{2+} channel current in α_o+/+ (○) and α_o−/− cells (▲, occluded by circles, and ■). Thirty-one α_o−/− and 21 α_o+/+ cells were analyzed. Current–voltage curves of α_o−/− cells fell into two groups: one with a $V_{1/2}$ of activation of −26 ± 1.5 mV and the other with $V_{1/2}$ of −12.7 ± 0.8 (mean ± SEM; $P < 0.001$). $V_{1/2}$ in +/+ cells was −14.2 ± 0.9 mV.

receptor in PC12 cells (52). In the "prepulse" protocol, receptor agonist is added to the bath, time is given to allow for installment of channel inhibition, and channel activity is recorded. First, the inhibited state is measured in response to a test pulse, and then it is remeasured after a strong depolarizing pulse to +80 mV or higher (prepulse), which relieves the inhibition exerted by receptor stimulation. Later studies have shown that inhibition is mediated by $G\beta\gamma$ and that loss of inhibition after the prepulse is simply because of dissociation of $G\beta\gamma$ from the channel's α_1 subunit. Repolarization allows for rebinding of $G\beta\gamma$ and reinstallment of the inhibition (e.g., refs. 28, 53, and 54). As shown in Fig. 4*C*, the Ca^{2+} current recorded in the presence of the μ-opioid receptor agonist DAMGO was "potentiated," i.e., uninhibited, by a prepulse. This proved the effective installment of channel inhibition through the $\beta\gamma$ arm of the G protein-coupled pathway.

Lack of Increase in Functionally Active (Free) $\beta\gamma$ Dimers in α_o−/− Cells. It has been shown that free $\beta\gamma$ dimers lead to

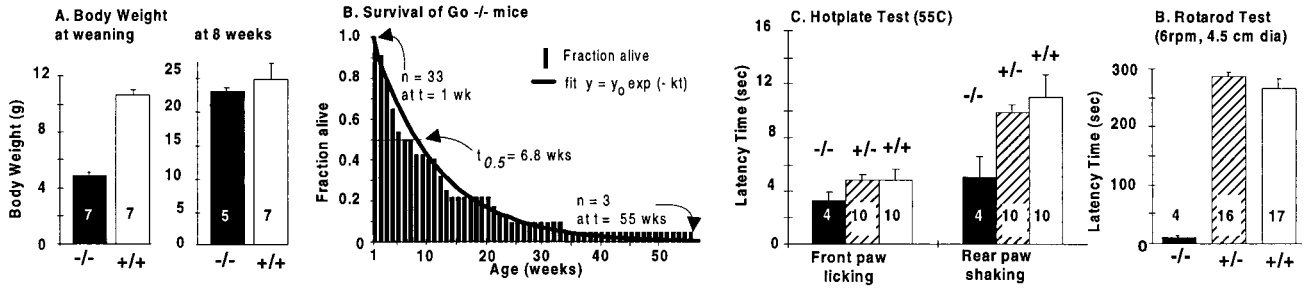

FIG. 3. Characteristics of G_o-deficient mice. (*A*) Body weight of littermates at 3 and 8 weeks of age. (*B*) Survival of 33 mice α_o−/− mice at 1 week old. (*C*) Hot-plate tests of −/−, +/−, and +/+ mice. (*D*) Time elapsed between start of rotation and fall off of mice from a 4.5-cm-diameter cylinder rotating at 6 rpm. For *A*, *C*, and *D*, data are the mean ± SEM.

development of prepulse potentiation in the absence of receptor agonist, so that prepulse potentiation becomes a sensitive test for the existence of functionally active $\beta\gamma$ dimers within the intact cell (14, 15). Fig. 4*C* shows the absence of prepulse potentiation before agonist addition in both $\alpha_o+/+$ and $\alpha_o-/-$ cells. This indicates that loss of the G_o α subunit did not lead to accumulation of an unbalanced excess of functionally active $\beta\gamma$ dimers.

Unimpaired Inhibition of Cardiac Adenylyl Cyclase Activity by a G_i/G_o-Coupled Receptor. In agreement with predictions from studies with partially reconstituted systems (55), with homogenates and membranes (56, 57), and with intact cells (58), it is now recognized that G_i proteins inhibit adenylyl cyclase activities through their activated α_i subunits. However, when compared with α_i subunits, the very similar α_o subunits do not appear to inhibit adenylyl cylcases (17, 18). The report of Valenzuela *et al.* (26), who in $\alpha_o-/-$ mice showed loss of carbachol-induced inhibition of isoproterenol-stimulated cardiac Ca^{2+} currents, raised the possibility that the M2 muscarinic receptor in ventricle cells might be acting by reducing the levels of cAMP, which stimulates this $G\beta\gamma$-insensitive channel, and that this reduction of cAMP levels might come about by activation of G_o. The possibility existed that loss of the carbachol action was caused by a loss in its ability to reduce adenylyl cyclase activty and thus that G_o might be acting as a G_i and inhibit adenylyl cyclase in cardiac ventriculocytes to the exclusion of G_i, perhaps because of a colocalization phenomenon. However, we found that carbachol (100 μM) inhibits cardiac adenylyl cyclase equally well in $\alpha_o+/+$ and $\alpha_o-/-$ homogenates [55 ± 3% inhibition for $\alpha_o+/+$ ($n = 4$) vs. 52 ± 4% ($n = 3$) for $\alpha_o-/-$; mean ± SD; data not shown). This indicated that whatever the mechanism is by which G_o-deficient mice lose muscarinic regulation of Ca^{2+} currents, it is not because of loss of regulation of cardiac adenylyl cyclase and points to yet another form of regulation of this effector system that is controlled by G_o by an unknown mechanism.

Motor Control. As reported (26), we also noted that $\alpha_o-/-$ mice have a generalized tremor. This tremor is accompanied by impairment of motor control. Thus, when placed on a rotating rod (rotarod) 4.5 cm in diameter, $\alpha_o-/-$ mice showed a marked deficiency in coordinated motor movement and a tendency to fall off, even from the stationary rod. None stayed on the rotating rod for more than 5 s (Fig. 3*D*). Likewise, when placed on a 1-m beam that was 1 inch wide (1 inch = 2.54 cm), $\alpha_o-/-$ mice generally did not walk along it or, when they did, they did so hesitantly and fell off after just a few paces.

Hyperactivity and Turning Behavior. Because of the impaired motor control, it was surprising to observe a higher level of activity in cages with $\alpha_o-/-$ mice. On closer observation, we noticed that $-/-$ mice appeared to be moving continuously. We thus placed $-/-$ mice individually into a box with the bottom covered with an approximately 1-inch-thick layer of washed and sterilized sand from the beach of Santa Monica, CA. Wild-type and $+/-$ mice behaved the same: walked for the most part along the sides of the box, stopped, reared, groomed, and inspected each corner. $G_o\alpha$ $-/-$ mice, in contrast, after a short delay during which they moved tentatively and slowly, gradually accelerated their walk, ignored corners, and were soon (within 1–2 min) running in circles. Depending on the individual, these circles were large and close to the periphery or, for 80% of the mice, changed continuously in diameter covering the complete surface of the box in a nonsystematic way. Thus, $-/-$ mice display a turning behavior that was not seen in wild-type or $+/-$ mice. We videotaped the movements of the mice, replayed the tape on a 9-inch television set, and traced the paths onto transparencies. Fig. 5 shows the paths of one $+/+$, one $+/-$, and one $-/-$ mouse and the superposition of the paths of five animals of each group. Once they had started turning, $-/-$ mice continued to do so at varying speeds. In a circular field 18 inches in diameter, the fastest (2155M) run 162.7 ± 20 circles (or ovals) (mean ± SD, $n = 3$) in 6 min (one every 2–3 s); the slowest made 25.5 ± 3.3 large circles in 6 min. Running is not totally continuous. The mice make short stops to defecate, resume running, stop shortly to inspect, and smell their droppings the next time by, and also stop for short grooming events—licking their coats and stroking their whiskers with their front paws. Otherwise $\alpha_o-/-$ mice run for hours on end. Short records of their turning behavior can be seen at http://rfh.anes.ucla.edu/~lutzb/realmice.htm. (requires REALPLAY software, which is down-loadable free of cost). The $\alpha_o-/-$ mice see: they avoid objects and other mice placed in their paths. Interactions with littermates ($-/-$, also running, $+/-$, or $+/+$) do occur and are friendly but hasty. $-/-$ animals eat and drink but do so also with haste. Neither $-/-$ females nor $-/-$ males have mated successfully. A histological examination of serial coronal sections of the brains of $\alpha_o-/-$ mice (fixed in 4% formalin, 5 μm thick at 100-μm intervals, stained with Luxol fast blue and counterstained with cresyl violet) revealed no obvious anatomical left–right differences.

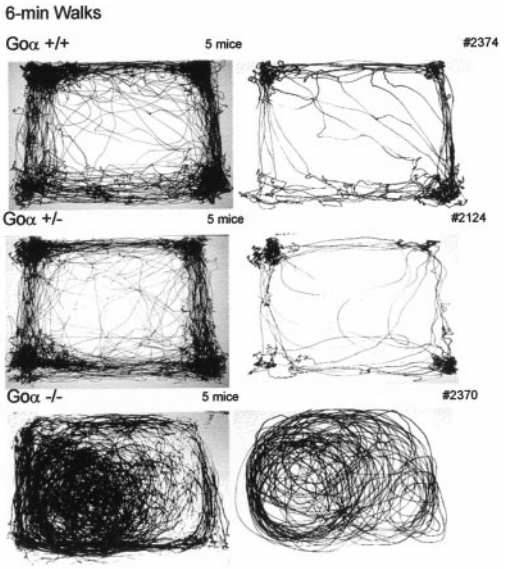

FIG. 5. Turning behavior of $\alpha_o-/-$ mice. Results from an open-field test in which a mouse is placed in a 13 × 17 inch box with a flat bottom covered with a 1-inch layer of sand (for details, see text). The lower superpositions show the movements of five $\alpha_o-/-$ mice (2065M, 2093F, 2155M, 2370M, and 2371F, where M is male and F is female). 2065M and 2371F walked almost exclusively along the sides of the box.

In summary, G_o-deficient mice show an array of defects that span from the molecular (e.g., unexpected defects and alterations in the regulation of Ca^{2+} currents) to the integrative (e.g., impaired motor control and extreme turning behavior). Elucidation of the biochemical and cellular mechanisms affected by loss of G_o is expected to lead to insights into cell signaling and homeostatic controls.

This work was supported in part by National Institutes of Health Grant DK-19318 to L.B.; a postdoctoral fellowship from the Medical Research Council, Ontario, Canada, to G.B.; a postdoctoral Fellowship of the Institute Nationale pour la Recherche Médicale to P.B.; and a postdoctoral fellowship from the Deutsche Forschungsgesellschaft to K.S. M.S.G. was the recipient of a Giannini Foundation Fellowship.

1. Neer, E. J., Lok, J. M. & Wolf, L. G. (1984) *J. Biol. Chem.* **259,** 14222–14229.
2. Huff, R. M., Axton, J. M. & Neer, E. J. (1985) *J. Biol. Chem.* **260,** 10864–10871.
3. Sternweis, P. C. & Robishaw, J. D. (1984) *J. Biol. Chem.* **259,** 13806–13813.

4. Cerione, R. A., Regan, J. W., Nakata, H., Codina, J., Benovic, J. L., Gierschick, P., Somers, R. L., Spiegel, A. M., Birnbaumer, L., Lefkowitz, R. J. & Caron, M. G. (1986) *J. Biol. Chem.* **261,** 3901–3909.
5. Florio, V. A. & Sternweis, P. C. (1985) *J. Biol. Chem.* **260,** 3477–3483.
6. Hescheler, J., Rosenthal, W., Trautwein, W. & Schultz, G. (1987) *Nature (London)* **325,** 445–447.
7. Kleuss, C., Hescheler, J., Ewel, C., Rosenthal, W., Schultz, G. & Wittig, B. (1991) *Nature (London)* **353,** 43–48.
8. Taussig, R., Sanchez, S., Rifo, M., Gilman, A. G., Belardetti, F. (1992) *Neuron* **8,** 799–809.
9. Chen, C. & Clarke, I. J. (1996) *J. Physiol.* **491,** 21–29.
10. Strittmatter, S. M., Valenzuela, D., Kennedy, T. E., Neer, E. J. & Fishman, M. C. (1990) *Nature (London)* **344,** 836–841.
11. Nishimoto, I., Okamoto, T., Matsuura, Y., Takahashi, S., Okamoto, T., Murayama, Y. & Ogata, E. (1993) *Nature (London)* **362,** 75–79.
12. Tsunoo, A., Yoshi, M. & Narahashi, T. (1986) *Proc. Natl. Acad. Sci. USA* **83,** 9832–9836.
13. Campbell, V., Berrow, N. & Dolphin, A. C. (1993) *J. Physiol.* **470,** 1–11.
14. Ikeda, S. R. (1996) *Nature (London)* **380,** 255–258.
15. Herlitze, S., Garcia, D. E., Mackie, K., Hille, B., Scheuer, T. & Catterall, W. A. (1996) *Nature (London)* **380,** 258–262.
16. Qin, N., Platano, D., Olcese, R., Stefani, E. & Birnbaumer, L. (1997) *Proc. Natl. Acad. Sci. USA* **94,** 8866–8871.
17. Wong, Y. H., Conklin, B. R. & Bourne, H. R. (1992) *Science* **255,** 339–342.
18. Taussig, R., Iñiguez-Lluhi, J. A. & Gilman, A. G. (1993) *Science* **261,** 218–221.
19. Kroll, S. D., Chen, J., De Vivo, M., Carthy, D. J., Buku, A., Premont, R. T. & Iyengar, R. (1992) *J. Biol. Chem.* **267,** 23183–23188.
20. Van Biesen, T., Hawes, B. E., Raymond, J. R., Luttrell, L. M., Koch, W. J. & Lefkowitz, R. J. (1996) *J. Biol. Chem.* **272,** 1266–1269.
21. Moriarty, T. M., Padrell, E., Corby, D. J., Omri, G., Landau, E. M. & Iyengar, R. (1990) *Nature (London)* **343,** 79–82.
22. VanDongen, A., Codina, J., Olate, J., Mattera, R., Joho, R., Birnbaumer, L. & Brown, A. M. (1988) *Science* **242,** 1433–1437.
23. Rudolph, U., Brabet, P., Kaplan, J., Hasty, P. Bradley, A. & Birnbaumer, L. (1993) *J. Recept. Res.* **13,** 619–637.
24. Rudolph, U., Finegold, M. J., Rich, S. S., Harriman, G. R., Srinivasan, Y., Brabet, P., Boulay, G., Bradley, A. & Birnbaumer, L. (1995) *Nat. Genet.* **10,** 143–150.
25. Offermans, S., Toombs, C. F., Hu, Y. H. & Simon, M. I. (1997) *Nature (London)* **389,** 183–186.
26. Valenzuela, D., Han, X., Mende, U., Fankhauser, C., Mashimo, H., Huang, H., Pfeffer, J., Neer, E. J. & Fishman, M. C. (1997) *Proc. Natl. Acad. Sci. USA* **94,** 1727–1732.
27. Bourinet, E., Soong, T. W., Stea, A. & Snutch, T. P. (1996) *Proc. Natl. Acad. Sci. USA* **93,** 1486–1491.
28. Zhang, J. F., Ellinor, P. T., Aldrich, R. W. & Tsien, R. W. (1996) *Neuron* **17,** 991–1003.
29. Tsukamoto, T., Toyama, R., Itoh, H., Kozasa, T., Matsuoka, M. & Kaziro, Y. (1991) *Proc. Natl. Acad. Sci. USA* **88,** 2974–2978.
30. Bertrand, P., Sanford, J., Rudolph, U., Codina, J. & Birnbaumer, L. (1990) *J. Biol. Chem.* **265,** 18576–18580.
31. Noel, J. P., Hamm, H. E. & Sigler, P. B. (1993) *Nature (London)* **366,** 654–663.
32. Graziano, M. P. & Gilman, A. G. (1989) *J. Biol. Chem.* **264,** 15475–15482.
33. Rudolph, U., Brabet, P., Hasty, P., Bradley, A. & Birnbaumer, L. (1993) *Transgenic Res.* **2,** 345–355.
34. Soriano, P., Montgomery, C., Geske, R. & Bradley, A. (1991) *Cell* **64,** 693–702.
35. Mansour, S. L., Thomas, K. R. & Capecchi, M. R. (1988) *Nature (London)* **336,** 348–352.
36. Codina, J., Grenet, D., Chang, K.-J. & Birnbaumer, L. (1991) *J. Receptor Res.* **11,** 587–601.
37. Rudolph, U., Spicher, K. & Birnbaumer, L. (1996) *Proc. Natl. Acad. Sci. USA* **93,** 3209–3214.
38. Sambrook, J., Fritsch, E. F. & Maniatis, T. (1989) *Molecular Cloning: A Laboratory Manual* (Cold Spring Harbor Lab. Press, Plainview, NY), 2nd Ed.
39. Feinberg, A. P. & Vogelstein, B. (1983) *Anal. Biochem.* **132,** 6–13.
40. Gold, M. S., Dastmalchi, S. & Levine, J. D. (1996) *Neuroscience* **71,** 265–275.
41. Khasar, S. G., Gold, M. S., Dastmalchi, S. & Levine, J. D. (1996) *Neurosci. Lett.* **218,** 17–20.
42. Itoh, H., Kozasa, T., Nagata, S., Nakamura, S., Katada, T., Ui, M., Iwai, S., Ohtsuka, E., Kawasaki, H., Suzuki, K. & Kaziro, Y. (1986) *Proc. Natl. Acad. Sci. USA* **83,** 3776–3780.
43. Jones, D. T. & Reed, R. R. (1987) *J. Biol. Chem.* **262,** 14241–14249.
44. VanMeurs, K. P., Angus, W., Lavu, S., Kung, H. F., Czarnecki, S. K., Moss, J. & Vaughan, M. (1987) *Proc. Natl. Acad. Sci. USA* **84,** 3107–3111.
45. Hsu, W. H., Rudolph, U., Sanford, J., Bertrand, P., Olate, J., Nelson, C., Moss, L. G., Boyd, A. E., III, Codina, J. & Birnbaumer, L. (1990) *J. Biol. Chem.* **265,** 11220–11226.
46. Strathmann, M., Wilkie, T. & Simon, M. I. (1990) *Proc. Natl. Acad. Sci. USA* **87,** 6477–6481.
47. Codina, J., Yatani, A., VonDongen, A. M. J., Padrell, E., Carty, D., Mattera, R., Brown, A. M., Iyengar, R. & Birnbaumer, L. (l990) in *G Proteins*, eds. Iyengar, R. & Birnbaumer, L. (Academic, San Diego), pp. 267–294.
48. Wilcox, M. D., Dingus, J., Balcueva, E. A., McIntire, W. E., Mehta, N. D., Schey, K. L., Robishaw, J. D. & Hildebrandt, J. D. (1995) *J. Biol. Chem.* **270,** 4189–4192.
49. Arbilla, S. & Langer, S. Z. (1978) *Nature (London)* **271,** 559–560.
50. Dolphin, A. C. (1996) *Trends Neurosci.* **19,** 35–43.
51. Marchetti, C., Carbone, E. & Lux, H. D. (1986) *Pflüegers Arch.* **406,** 104–111.
52. Bean, B. P. (1989) *Nature (London)* **340,** 153–156.
53. Lipscombe, D., Kongsamut, S. & Tsien, R. W. (1989) *Nature (London)* **340,** 639–642.
54. Lopez, H. S. & Brown, A. M. (1991) *Neuron* **7** 1061–1068.
55. Hildebrandt, J. D., Codina, J. & Birnbaumer, L. (1984) *J. Biol. Chem.* **259,** 13178–13185.
56. Toro, M.-J., Montoya, E. & Birnbaumer, L. (1987) *Mol. Endocrinol.* **1,** 669–676.
57. Hildebrandt, J. D. & Kohnken, R. E. (1990) *J. Biol. Chem.* **265,** 9825–9830.
58. Wong, Y. H., Federman, A., Pace, A. M., Zachary, I, Evans, T., Pouysségur & Bourne, H. R. (1991) *Nature (London)* **351,** 63–65.